

Article

# Biogenic Fe(II-III) Hydroxycarbonate Green Rust Enhances Nitrate Removal and Decreases Ammonium Selectivity during Heterotrophic Denitrification

Georges Ona-Nguema <sup>1,\*</sup>, Delphine Guerbois <sup>1</sup>, Céline Pallud <sup>2</sup>, Jessica Brest <sup>1</sup>, Mustapha Abdelmoula <sup>3</sup>  and Guillaume Morin <sup>1</sup>

<sup>1</sup> Faculté des Sciences et Ingénierie, Campus Pierre & Marie Curie, Institut de Minéralogie, de Physique des Matériaux et de Cosmochimie (IMPMC), Sorbonne Université-CNRS UMR 7590-Muséum National d'Histoire Naturelle-IRD UMR 206, 4 place Jussieu, F-75005 Paris, France; d.guerbois@live.fr (D.G.); jessica.brest@sorbonne-universite.fr (J.B.); guillaume.morin@sorbonne-universite.fr (G.M.)

<sup>2</sup> Policy and Management, Department of Environmental Science, University of California, 130 Mulford Hall, MC 3114, Berkeley, CA 94720-3114, USA; cpallud@berkeley.edu

<sup>3</sup> Université de Lorraine, CNRS, LCPME, F-54000 Nancy, France; mustapha.abdelmoula@univ-lorraine.fr

\* Correspondence: georges.ona\_nguema@sorbonne-universite.fr; Tel.: +33-1-44-27-72-47

Received: 6 August 2020; Accepted: 11 September 2020; Published: 16 September 2020



**Abstract:** Nitrification-denitrification is the most widely used nitrogen removal process in wastewater treatment. However, this process can lead to undesirable nitrite accumulation and subsequent ammonium production. Biogenic Fe(II-III) hydroxycarbonate green rust has recently emerged as a candidate to reduce nitrite without ammonium production under abiotic conditions. The present study investigated whether biogenic iron(II-III) hydroxycarbonate green rust could also reduce nitrite to gaseous nitrogen during bacterial nitrate reduction. Our results showed that biogenic iron(II-III) hydroxycarbonate green rust could efficiently decrease the selectivity of the reaction towards ammonium during heterotrophic nitrate reduction by native wastewater-denitrifying bacteria and by three different species of *Shewanella*: *S. putrefaciens* ATCC 12099, *S. putrefaciens* ATCC 8071 and *S. oneidensis* MR-1. Indeed, in the absence of biogenic hydroxycarbonate green rust, bacterial reduction of nitrate converted 11–42% of the initial nitrate into ammonium, but this value dropped to 1–28% in the presence of biogenic hydroxycarbonate green rust. Additionally, nitrite accumulation did not exceed the 2–13% in the presence of biogenic hydroxycarbonate green rust, versus 0–28% in its absence. Based on those results that enhance the extent of denitrification of about 60%, the study proposes a water treatment process that couples the bacterial nitrite production with the abiotic nitrite reduction by biogenic green rust.

**Keywords:** biogenic hydroxycarbonate green rust; heterotrophic denitrification; *Shewanella putrefaciens* ATCC 12099; *Shewanella putrefaciens* ATCC 8071; *Shewanella oneidensis* MR-1; selectivity; ammonium; nitrate; nitrite; native wastewater-denitrifying consortia

## 1. Introduction

Nitrogen is present in the environment as organic (e.g., proteins, amino acids, DNA, RNA) and inorganic forms, including soluble (ammonium 'NH<sub>4</sub><sup>+</sup>', nitrate 'NO<sub>3</sub><sup>-</sup>', nitrite 'NO<sub>2</sub><sup>-</sup>') and gaseous (nitric oxide 'NO', nitrous oxide 'N<sub>2</sub>O', di-nitrogen 'N<sub>2</sub>') compounds. When present at large concentrations in surface waters, inorganic nitrogen compounds are highly toxic to humans, plants and fauna [1–4], and are responsible for ecosystem eutrophication [5,6]. In anoxic environments, numerous fermenting and non-fermenting microorganisms are capable of converting nitrate into ammonium by dissimilatory nitrate reduction to ammonium (DNRA) [7] (Figure 1). As a result of

nitrification and denitrification processes, nitrite accumulation can be observed in oxic and anoxic environments, particularly in sensitive zones [1,8,9]. Once ingested, nitrite can be transformed into carcinogenic N-nitroso compounds, which are suspected to be responsible for some gastric cancers, and is responsible for the formation of methaemoglobin, leading to hypoxia and blue-baby syndrome [1].

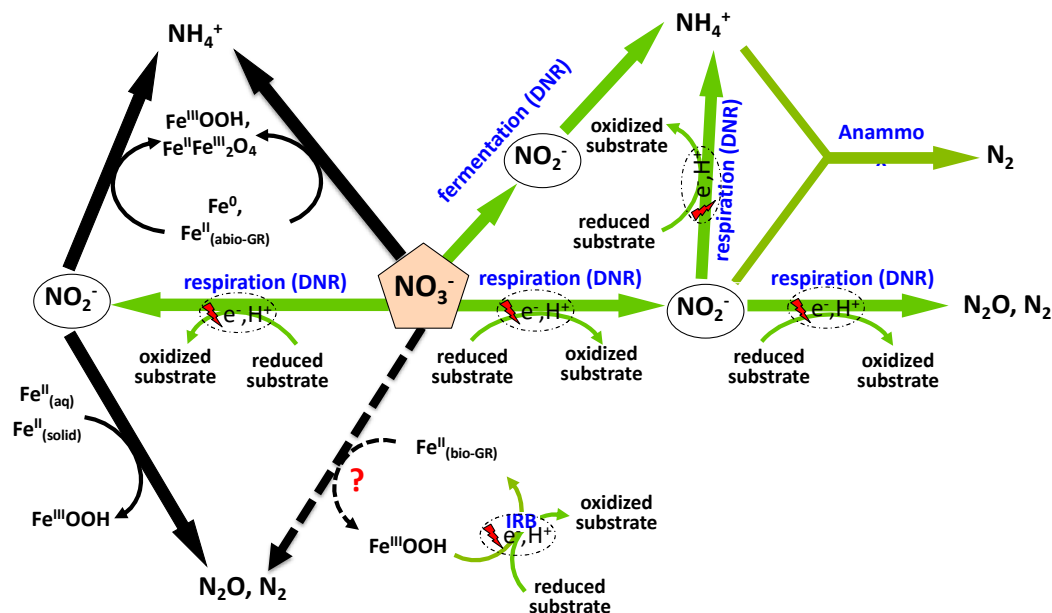


**Figure 1.** Conceptual diagram of the major biotic and abiotic processes involved in nitrogen reduction. Green and black arrows represent biotic and abiotic reactions, respectively. IRB: iron-respiring bacteria,  $\text{Fe}^{\text{III}}\text{OOH}$ : ferric oxyhydroxides,  $\text{Fe}^{\text{II}}\text{Fe}^{\text{III}}_2\text{O}_4$ : magnetite,  $\text{Fe}^{\text{II}}(\text{abio-GR})$ : abiotic green rust,  $\text{Fe}^{\text{II}}(\text{bio-GR})$ : biogenic hydroxycarbonate green rust, reduced substrate: organic or inorganic electron donors, DNR: dissimilatory nitrate/nitrite reduction, Anammox: anaerobic ammonium oxidation.

On the other hand, ammonium is a highly reactive compound with significant cytotoxicity. In mammals, high ammonium levels (up to  $35 \mu\text{mol/L}$ ) can provoke a large diversity of pathologies, such as the hepatic encephalopathy that results in a swelling of the brain [2,10]. Consequently, wastewater and drinking water treatments include nitrogen removal processes. Nitrogen pollution in wastewater consists mainly of organic and ammoniacal nitrogen (i.e., Kjeldahl nitrogen), and the fraction of organic nitrogen is fully converted to ammonium by ammonification during wastewater transportation. The most widely used process for nitrogen removal in wastewater treatment plants (WWTP) is a system that combines nitrification and denitrification reactions. Nitrification is a two-step process that takes place under oxic conditions, where autotrophic nitrifying bacteria couple the oxidation of ammonium to nitrite, then to nitrate, with the reduction of molecular oxygen. Denitrification takes place under anoxic conditions, where heterotrophic bacteria couple the oxidation of organic matter to  $\text{HCO}_3^-$  with the reduction of nitrate to nitrite then to nitrogen gas ( $\text{N}_2$ ) and to a lesser extent into nitrous oxide ( $\text{N}_2\text{O}$ ) [11] (Figure 1).

The full conversion of nitrate into gaseous nitrogen species depends on the biodegradability of the wastewater, which could be determined by the ratio of chemical oxygen demand (COD) to biochemical oxygen demand (BOD). The biodegradability of the wastewater increases with decreasing COD:BOD ratio. Indeed, agro-food industrial and domestic wastewater influents are the most biodegradable sewage with average values of COD:BOD ratio of  $1.9 \pm 0.4$  (Table 1) [12], and  $2.4 \pm 0.8$  (Table 1) [13–20], respectively. In contrast, chemical industrial wastewater influents are less biodegradable and their COD:BOD ratio is generally up to 4 (Table 1) [21–24]. Consequently, a costly strategy in WWTP involves the addition of highly biodegradable carbon sources, such as methanol and/or acetate, in order to fully achieve the denitrification process under anoxic conditions [11]. However, physical methods for nitrate

removal such as reverse osmosis, ion exchange or electro-dialysis that are especially used for drinking water treatment, are costly and generate waste brines [25].

**Table 1.** Biodegradability of wastewater with respect to organic compounds: comparison between agro-food industry, domestic, and chemical industry wastewater.

Origin of Carbon Compounds	COD (mg O <sub>2</sub> /L)	BOD (mg O <sub>2</sub> /L)	COD/BOD Ratio	Average ± sd	References
Agro-food industry	4018	2045	2.0		[26]
Agro-food industry	50,000	25,000	2.0		[27]
Agro-food industry	1950	900	2.2	1.9 ± 0.4	[28]
Agro-food industry	7800	3450	2.3		[29]
Agro-food industry	5750	5000	1.2		[30]
Agro-food industry	10,496	6300	1.7		[31]
Domestic wastewater	925	440	2.1		[18]
Domestic wastewater	912	289	3.2		[19]
Domestic wastewater	285.2	71.4	4.0		[17]
Domestic wastewater	960	450	2.1	2.4 ± 0.8	[20]
Domestic wastewater	1420	900	1.6		[16]
Domestic wastewater	300	160	1.9		[13]
Domestic wastewater	522	208	2.5		[15]
Domestic wastewater	550	250	2.2		[14]
Chemical industry	340.7	8.9	38.5		[22]
Chemical industry	2912	150	19.4	30 ± 23	[21]
Chemical industry	495	127.5	3.9		[24]
Chemical industry	4566	80	57.1		[23]

Alternatively, nitrate can be abiotically reduced by zero-valent iron, Fe(0), forming ammonium in a fast reaction (Figure 1) [32–35]. During the reaction of Fe(0) with nitrate, corrosion products of iron are formed, including green rusts (GR), which are mixed layered Fe(II)-Fe(III) hydroxysalts [36,37]. Few studies have demonstrated nitrate reduction by abiotic hydroxyfluoride green rust abio-GR(F) [38], hydroxysulfate green rust abio-GR(SO<sub>4</sub>) [39], and hydroxychloride green rust abio-GR(Cl) [40] with a systematic conversion of nitrate into ammonium (Figure 1). Recently, a study by Guerbois et al. [41] showed that at neutral initial pH nitrite could be reduced by biogenic mixed-valent iron(II-III) hydroxycarbonate green rust bio-GR(CO<sub>3</sub>) forming gaseous nitrogen species without ammonium production (Figure 1). The latter study provided the first evidence of the formation of biogenic hydroxy-nitrite green rust bio-GR(NO<sub>2</sub>), a new type of green rust 1, thereby confirming the hypothetical reaction scheme of nitrate reduction by abio-GR(F) proposed by Choi and Batchelor [38], and indicating that the mechanism of nitrite reduction by bio-GR(CO<sub>3</sub>) involves both external and internal reaction sites. Such a mechanism could explain the higher reactivity of green rust with respect to nitrite, compared to other mineral substrates possessing only external reactive sites. Further research is thus required to decrease nitrite and ammonium production in both biotic and abiotic denitrification processes.

The abiotic oxidation and reduction reactions, represented by dashed black arrows in Figure 1, are a hypothetical full conversion of nitrate ions to gaseous nitrogen by biogenic hydroxycarbonate green rusts produced upon the bioreduction of ferric oxyhydroxides by iron-respiring bacteria (IRB). Such an abiotic reduction of nitrate to N<sub>2</sub>/N<sub>2</sub>O by biogenic green rusts without ammonium production has never been studied and is explored in the present work.

The current study shows that biogenic mixed-valent iron(II-III) hydroxycarbonate green rust can efficiently reduce nitrite and decrease ammonium selectivity during bacterial nitrate reduction by three different strains of *Shewanella*, and by a native bacterial consortium from wastewater. On the basis of those results, the study proposes to couple bacterial nitrate reduction to nitrite production with abiotic nitrite reduction by biogenic hydroxycarbonate green rusts to gaseous nitrogen species as a water treatment process.

## 2. Materials and Methods

Biogenic hydroxycarbonate green rusts production. The biogenic hydroxycarbonate green rusts were produced from the bioreduction of ferric oxyhydroxycarbonate or of lepidocrocite by *Shewanella putrefaciens* ATCC 12099 at neutral pH in the presence of sodium methanoate as an electron donor, and of anthraquinone-2,6-disulfonate (AQDS) as an electron shuttle under anoxic conditions. ATCC refers to as the American Type Culture Collection. The full description of the protocol of biogenic hydroxycarbonate green rusts production is detailed in our previous study by Guerbois et al. [41].

Transmission Mössbauer Spectroscopy analysis. Subsamples (10 mL) were taken from the well-homogenized biogenic hydroxycarbonate green rust suspensions in the glove box under a nitrogen atmosphere; iron particles were concentrated by filtration (0.45- $\mu\text{m}$  pore size) and quickly transferred to the cryostat under inert He atmosphere before measuring at 77 K. Transmission Mössbauer analysis was performed with a Mössbauer cryostat equipped with a vibration isolation stand manufactured by Cryo Industries of America (Macungie, PA, USA), utilizing a constant acceleration Mössbauer spectrometer with a 50 mCi source of  $^{57}\text{Co}$  in Rh and calibrated with a 25  $\mu\text{m}$  thick  $\alpha$ -iron foil at ambient temperature. The spectra were fit with the software Recoil<sup>TM</sup> using Lorentzian or pseudo-Voigt line shapes. The Fe(II)/Fe(III) ratios of these biogenic hydroxycarbonate green rusts ranged from 1.0 to 1.2.

Denitrification batches. Before investigating the effects of bio-GR(CO<sub>3</sub>) on microbial nitrate reduction, the reactivity of bio-GR(CO<sub>3</sub>) with respect to nitrate was firstly assessed at three different pH values ( $6.5 \pm 0.1$ ,  $7.5 \pm 0.1$  and  $10.0 \pm 0.1$ ) (Table 2) to determine if the bio-GR(CO<sub>3</sub>) particles are capable of reducing nitrate ions. Three distinct sets of bacterial incubations were performed at room temperature and at pH  $7.5 \pm 0.1$  (Table 2): (1) nitrate and nitrite reduction by three *Shewanella* strains, (2) addition of nitrate or nitrite solution to wastewater influents containing native wastewater-denitrifying consortia, and (3) mixed denitrification by both bacteria and bio-GR(CO<sub>3</sub>). In the abiotic experiments, 0.1 g of bio-GR(CO<sub>3</sub>) was suspended in the media, and the reaction was started by the addition of a NaNO<sub>3</sub> solution (300 mM). The final volume of each experiment was equal to 60 mL. Biotic denitrification experiments were performed with *S. putrefaciens* ATCC 12099, *S. putrefaciens* ATCC 8071 and *S. oneidensis* MR-1, which were obtained from the Institut Pasteur collection (Collection de l'Institut Pasteur, CIP). MR-1 refers to as "manganese reduction" because the first strain of *S. oneidensis* (formerly *Alteromonas putrefaciens*) was originally isolated from the anoxic sediments of Oneida Lake, New York, as a manganese reducer. The inocula of the three *Shewanella* strains were prepared as described by Ona-Nguema et al. [42–44]. The bacterial density of inoculum was determined by the number of colony-forming units (CFU). Culture media of biotic experiments were composed of basic medium, methanoate (48.5 mM) as the sole electron donor, and nitrate or nitrite as electron acceptors for which the starting concentrations in all experiments are indicated in Table 2. The composition of the basic medium used in the biotic experiments performed with *Shewanella* spp. was as follows: NH<sub>4</sub>Cl (22.0 mM), KCl (1.2 mM), CaCl<sub>2</sub> (0.692 mM), nitrilotriacetic acid (0.71 mM), NaCl (1.51 mM), MnSO<sub>4</sub>·H<sub>2</sub>O (0.27 mM), MgSO<sub>4</sub>·7H<sub>2</sub>O (1.10 mM), ZnSO<sub>4</sub>·7H<sub>2</sub>O (0.086 mM), FeSO<sub>4</sub>·7H<sub>2</sub>O (0.032 mM), Na<sub>2</sub>MoO<sub>4</sub>·2H<sub>2</sub>O (0.0095 mM), Na<sub>2</sub>WO<sub>4</sub>·2H<sub>2</sub>O (0.007 mM), NiCl<sub>2</sub> anhydrous (0.009 mM), CuSO<sub>4</sub>·5H<sub>2</sub>O (0.0036 mM), AlK(SO<sub>4</sub>)<sub>2</sub>·12H<sub>2</sub>O (0.0019 mM), H<sub>3</sub>BO<sub>3</sub> (0.0146 mM), CoSO<sub>4</sub>·7H<sub>2</sub>O (0.0381 mM). The starting NH<sub>4</sub><sup>+</sup> concentration in the basic medium was equal to 128.35 mg-N L<sup>-1</sup>; this value was considered as the baseline and had been subtracted in each experiment. The incubations were started by adding an inoculum of *S. putrefaciens* ATCC 12099, *S. putrefaciens* ATCC 8071 or *S. oneidensis* MR-1 of  $7 \times 10^9$  CFU/mL as a final bacterial density (Table 2). For the assays carried out in the presence of both bacteria and bio-GR(CO<sub>3</sub>), experimental conditions were similar to those of bacterial incubations, but 0.1 g of bio-GR(CO<sub>3</sub>) was added to the medium (Table 2).

**Table 2.** Initial conditions of biotic and abiotic experiments. All experiments performed with strains ATCC 12099, ATCC 8071, and MR-1 were carried out with 48.5 mM of methanoate as the sole electron donor and at room temperature under anoxic conditions.

Experiments	Mass of Bio-GR (g)	[NO <sub>3</sub> <sup>-</sup> ] (mg-N L <sup>-1</sup> )	[NO <sub>2</sub> <sup>-</sup> ] (mg-N L <sup>-1</sup> )	[NH <sub>4</sub> <sup>+</sup> ] (mg-N L <sup>-1</sup> )	Initial pH	Bacterial Density (CFU mL <sup>-1</sup> )
<sup>1</sup> bio-GR + nitrate	0.1	75(2)	0	0	6.5	0
<sup>1</sup> bio-GR + nitrate	0.1	76(0)	0	0	7.5	0
<sup>1</sup> bio-GR + nitrate	0.1	76(0)	0	0	10.0	0
<sup>2</sup> Strain ATCC 12099 + nitrate	–	89(4)	0	0	7.5	7 × 10 <sup>9</sup>
<sup>1</sup> bio-GR +	0.1	83(0)	0	0	7.5	7 × 10 <sup>9</sup>
Strain ATCC 12099 + nitrate	–	0	58(14)	0	7.5	7 × 10 <sup>9</sup>
<sup>1</sup> Strain ATCC 12099 + nitrite	–	83(3)	0	0	7.5	7 × 10 <sup>9</sup>
<sup>2</sup> Strain ATCC 8071 + nitrate	–	83(0)	0	0	7.5	7 × 10 <sup>9</sup>
<sup>1</sup> bio-GR +	0.1	83(0)	0	0	7.5	7 × 10 <sup>9</sup>
Strain ATCC 8071 + nitrate	–	0	66(13)	0	7.5	7 × 10 <sup>9</sup>
<sup>1</sup> Strain ATCC 8071 + nitrite	–	92(4)	0	0	7.5	7 × 10 <sup>9</sup>
<sup>1</sup> bio-GR +	0.1	83(0)	0	0	7.5	7 × 10 <sup>9</sup>
Strain MR-1 + nitrate	–	0	72(2)	0	7.5	7 × 10 <sup>9</sup>
<sup>2</sup> Strain MR-1 + nitrite	–	73	2.2	55	7.5	n.d.
<sup>3</sup> Wastewater influents + nitrate	0.1	84	0.1	52	7.5	n.d.
<sup>3</sup> bio-GR + nitrate +	–	0	74	61	7.5	n.d.
Wastewater influents	0.1	0	77(0)	71(18)	7.5	n.d.
<sup>3</sup> Wastewater influents + nitrite	–	0	77(0)	71(18)	7.5	n.d.
<sup>2</sup> bio-GR + nitrite +	0.1	0	77(0)	71(18)	7.5	n.d.
Wastewater influents	–	0	77(0)	71(18)	7.5	n.d.

<sup>1</sup> Triplicate experiments; <sup>2</sup> duplicate experiments; <sup>3</sup> single experiments; n.d.: not determined; mean values obtained from duplicate or triplicate experiments are indicated, with standard deviations given in parentheses.

All experiments were performed in a glove box under an argon atmosphere in sealed glass bottles at pH 7.5 ± 0.1. All solutions were prepared with O<sub>2</sub>-free Milli-Q water obtained by bubbling argon at 80 °C for 45 min, and they were sterilized by autoclaving, except for the methanoate solution that was sterilized by filtration through 0.2 µm cellulose nitrate filters. Bottles were shaken during the course of experiments using a rotary tube mixer with a disc. Experiments performed with and without bio-GR(CO<sub>3</sub>) using pure bacterial strains were monitored for two hours; for bacterial assays carried out in the absence of bio-GR(CO<sub>3</sub>), subsamples were taken approximately every 10 min during the first hour, then every 30 min for analyses, while in the presence of bio-GR(CO<sub>3</sub>), subsamples were taken every 30 min. For experiments performed with wastewater containing native wastewater-denitrifying consortia, 6–7 subsamples were taken during the first day of incubation, then one per day for four or five days.

**Solution analysis.** In all experiments, suspension samples were collected for total Fe(II), and dissolved NO<sub>3</sub><sup>-</sup>, NO<sub>2</sub><sup>-</sup> and NH<sub>4</sub><sup>+</sup> analyses. For total Fe(II) measurement, 0.5 mL of sample was dissolved in 0.5 mL HCl 1 M. After the dissolution of samples, colorimetric Fe(II) measurements were performed in 15 mL iron-free plastic vials by addition of 0.1 mL of sample to 2 mL of a stock solution containing 11.4 mM 1,10-phenanthroline, 227.3 mM Glycocoll and 9.1 mM nitrilotriacetic acid solution, and 7.9 mL of Milli-Q water were added to reach a final volume of 10 mL (protocol modified by Ona-Nguema from Fadrus and Maly [45]); spectrophotometric measurements were done at 510 nm using a visible spectrophotometer (Novaspec Plus, Biochrom, Holliston, MA, USA). Dissolved NO<sub>3</sub><sup>-</sup>, NO<sub>2</sub><sup>-</sup> and NH<sub>4</sub><sup>+</sup> concentrations were measured by ion chromatography (ISC 3000, DIONEX, Sunnyvale, CA, USA) after 0.22 µm filtration. According to units generally used in the water treatment literature, all concentrations values are given in mg L<sup>-1</sup> N-NO<sub>3</sub><sup>-</sup>, N-NO<sub>2</sub><sup>-</sup> or N-NH<sub>4</sub><sup>+</sup>, which correspond to weight concentrations of N dissolved in the form of NO<sub>3</sub><sup>-</sup>, NO<sub>2</sub><sup>-</sup> and NH<sub>4</sub><sup>+</sup>.

**Computations-Experiments with three *Shewanella* strains.** Bacterial nitrate reduction followed a two-step regime. The initial rates of bacterial nitrate reduction were calculated using a linear regression fitting procedure in the time interval between the starting and the end of the first step of the reaction, i.e., between time zero and 90 min for ATCC 12099 and ATCC 8071, between time zero and 30 min for MR-1, and between time zero and 60 min for all experiments carried out in the presence of bio-GR(CO<sub>3</sub>).

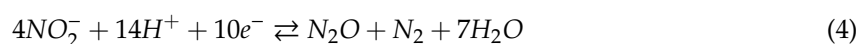
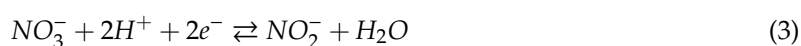


Computations-Experiments with wastewater influents. A pseudo-first-order kinetic model was used to fit experimental data of bacterial nitrate and nitrite reduction over time. The corresponding exponential decay can be expressed by Equations (1) and (2) as follows:

$$\frac{d[NO_x^-]}{dt} = -k_{obs} \cdot [NO_x^-] \quad (1)$$

$$[NO_x^-]_t = [NO_x^-]_0 \cdot e^{-k_{obs} \cdot t} \quad (2)$$

where  $[NO_x^-]_t$  is the concentration of  $NO_3^-$  or  $NO_2^-$  at time  $t$ ,  $[NO_x^-]_0$  is the initial concentration of  $NO_3^-$  or  $NO_2^-$ , and  $k_{obs}$  is the first-order rate constant. For data fitting, we considered (1) that nitrite is an obligatory reaction intermediate product in denitrification (Equations (3) and (4)), and (2) that the reduction reaction of nitrate and nitrite is independent of electron donor and nutrient concentrations as these substrates are in excess in wastewater influents. All nitrate and nitrite reduction can then be modeled as a pseudo-first-order reaction.



Computations-Ammonium and nitrite selectivity. The selectivity of the reaction towards ammonium  $S(NH_4^+)$  is the ratio between the fraction of ammonium produced  $R(NH_4^+)$  to that of nitrate removed, as described by Ruby et al. [46]. The selectivity of the reaction towards nitrite  $S(NO_2^-)$  was calculated as described for ammonium.  $X(NO_3^-)_t$  and  $X(NO_2^-)_t$  correspond to the fraction of nitrate or nitrite removed in experiments performed with nitrate or nitrite in the starting solutions, respectively;  $R(NH_4^+)_t$  is the ratio between the concentration of ammonium produced and that of nitrate or nitrite initially added to each experiment;  $R(NO_2^-)_t$  is the ratio between the concentration of nitrite produced and that of nitrate initially added to each experiment.

$$S(NH_4^+)_t = \frac{R(NH_4^+)_t}{X(NO_3^-)_t} \quad (5)$$

$$S(NH_4^+)_t = \frac{([NH_4^+]_t - [NH_4^+]_0) / [NO_3^-]_0}{([NO_3^-]_0 - [NO_3^-]_t) / [NO_3^-]_0} \quad (6)$$

$$S(NH_4^+)_t = \frac{([NH_4^+]_t - [NH_4^+]_0)}{([NO_3^-]_0 - [NO_3^-]_t)} \quad (7)$$

### 3. Results

#### 3.1. Characterization of Biogenic Iron(II-III) Hydroxycarbonate Green Rust Samples

All biogenic hydroxycarbonate green rusts produced from the bioreduction of ferric oxyhydroxycarbonate or of lepidocrocite in *Shewanella putrefaciens* cultures have been characterized by Mössbauer spectroscopy. Here we show an example of the 77 K transmission Mössbauer spectrum of a biogenic sample (Figure 2), which can be reasonably fitted with three paramagnetic quadrupole doublets  $D_1$ ,  $D_2$  and  $D_3$ . The doublets  $D_1$  (51%) and  $D_2$  (3%) showing large hyperfine parameters, i.e., center shift (1.25 and 1.26 mm s<sup>-1</sup>, respectively) and quadrupole splitting (2.88 and 2.39 mm s<sup>-1</sup>, respectively) correspond to high-spin Fe<sup>2+</sup> in octahedral sites. In contrast, the doublet  $D_3$  (46%), with small center shift (0.42 mm s<sup>-1</sup>) and quadrupole splitting (0.41 mm s<sup>-1</sup>), is due to high-spin Fe<sup>3+</sup> in octahedral sites. These Mössbauer hyperfine parameters are characteristic of hydroxycarbonate green rust. The Fe(II)/Fe(III) ratio determined from the fit of the present Mössbauer spectrum is equal to 1.2.

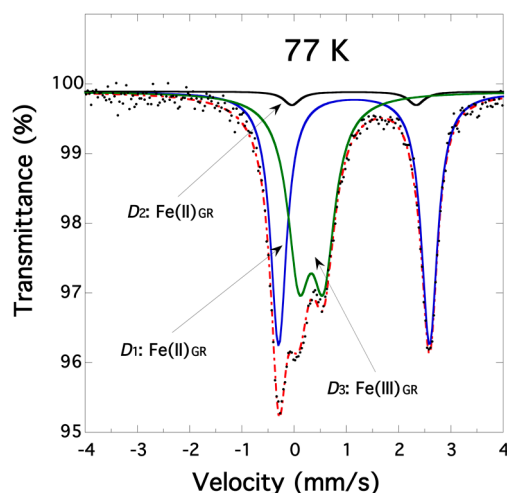


**Figure 2.** Transmission Mössbauer spectrum for biogenic hydroxycarbonate green rust recorded at 77 K. Experimental and fit curves are displayed as dotted black and dashed red lines, respectively. The fit components displayed as plain lines correspond to three doublets  $D_1$ ,  $D_2$  and  $D_3$ .

### 3.2. Nitrate Reduction in Axenic Cultures of *Shewanella* spp. with and without Biogenic Iron(II-III) Hydroxycarbonate Green Rust

Results reveal that nitrate was fully reduced in less than 2 h by three strains of *Shewanella* both in the absence (Figure 3a–c) and presence (Figure 3d–f) of bio-GR(CO<sub>3</sub>). In the absence of bio-GR(CO<sub>3</sub>), nitrate was fully reduced after 60–90 min for *Shewanella putrefaciens* strains ATCC 12099 and ATCC 8071 (Figure 3a,b), and after 20–30 min of incubation for *S. oneidensis* strain MR-1 (Figure 3c). In contrast, suspensions containing bio-GR(CO<sub>3</sub>) particles alone were not capable of reducing nitrate ions at pH 6.5, 7.5 or 10.0 (Figure 4). Moreover, the measurements of dissolved Fe(II) concentrations, which are in equilibrium with bio-GR(CO<sub>3</sub>) particles, indicate that Fe(II) contents are pH-dependent; the highest average value  $6.9 \pm 0.1$  mM being obtained at pH 6.5 compared to pH 7.5 and 10.0 for which only  $1.9 \pm 0.1$  mM and  $0.7 \pm 0.2$  mM of dissolved Fe(II) is observed, respectively (Figure 4).

All nitrate reduction curves followed a two-step regime. Initial rates calculated during the first step using a linear regression equation showed that nitrate reduction rates were higher in the presence of bio-GR(CO<sub>3</sub>) ( $-75 \pm 8$  mg-N L<sup>-1</sup> h<sup>-1</sup>,  $r^2 = 0.98 \pm 0.02$ ) than without it ( $-55 \pm 4$  mg-N L<sup>-1</sup> h<sup>-1</sup>,  $r^2 = 0.96 \pm 0.02$ ) (Figure 3a,b,d,e and Figure 5a,b,d,e) for the strains ATCC 12099 and ATCC 8071. However, for *S. oneidensis* strain MR-1 nitrate reduction rate was higher in the absence of bio-GR(CO<sub>3</sub>) ( $-186 \pm 10$  mg-N L<sup>-1</sup> h<sup>-1</sup>,  $r^2 = 0.98 \pm 0.01$ ) than with it ( $-81 \pm 1$  mg-N L<sup>-1</sup> h<sup>-1</sup>,  $r^2 = 0.92 \pm 0.04$ ) (Figure 3c,f and Figure 5c,f). Our results also showed that nitrite was produced as a reaction intermediate nitrogen species under all experimental conditions, the highest nitrite concentration being observed when nitrate was almost fully reduced (Figure 3). After 120 min of incubation in the presence of bio-GR(CO<sub>3</sub>), the selectivity of the reaction towards nitrite significantly decreased from 12 to 2%, and from 44 to 13%, respectively for strain ATCC 12099 and strain ATCC 8071 (Student's *t*-test, *p*-value < 0.05; Figure 6; Table 3). In contrast for strain MR-1, the selectivity of the reaction towards nitrite was significantly lower in the absence of bio-GR(CO<sub>3</sub>) ( $S(\text{NO}_2^-) = 0\%$ ) than in its presence ( $S(\text{NO}_2^-) = 7\%$ ) (Student's *t*-test, *p*-value < 0.05; Figure 6; Table 3). Nitrite accumulation was overall lower in the presence of bio-GR(CO<sub>3</sub>) than without it (Figure 3). In addition, after 120 min of incubation, results showed that in the presence of bio-GR(CO<sub>3</sub>), the selectivity of the reaction towards ammonium decreased significantly from  $37 \pm 5\%$  to  $28 \pm 3\%$ ,  $31 \pm 3\%$  to  $11 \pm 1\%$ , and from  $42 \pm 12\%$  to  $4 \pm 6\%$ , respectively for strains ATCC 12099, ATCC 8071 and MR-1 (Student's *t*-test, *p*-value < 0.05; Figure 6; Table 3).

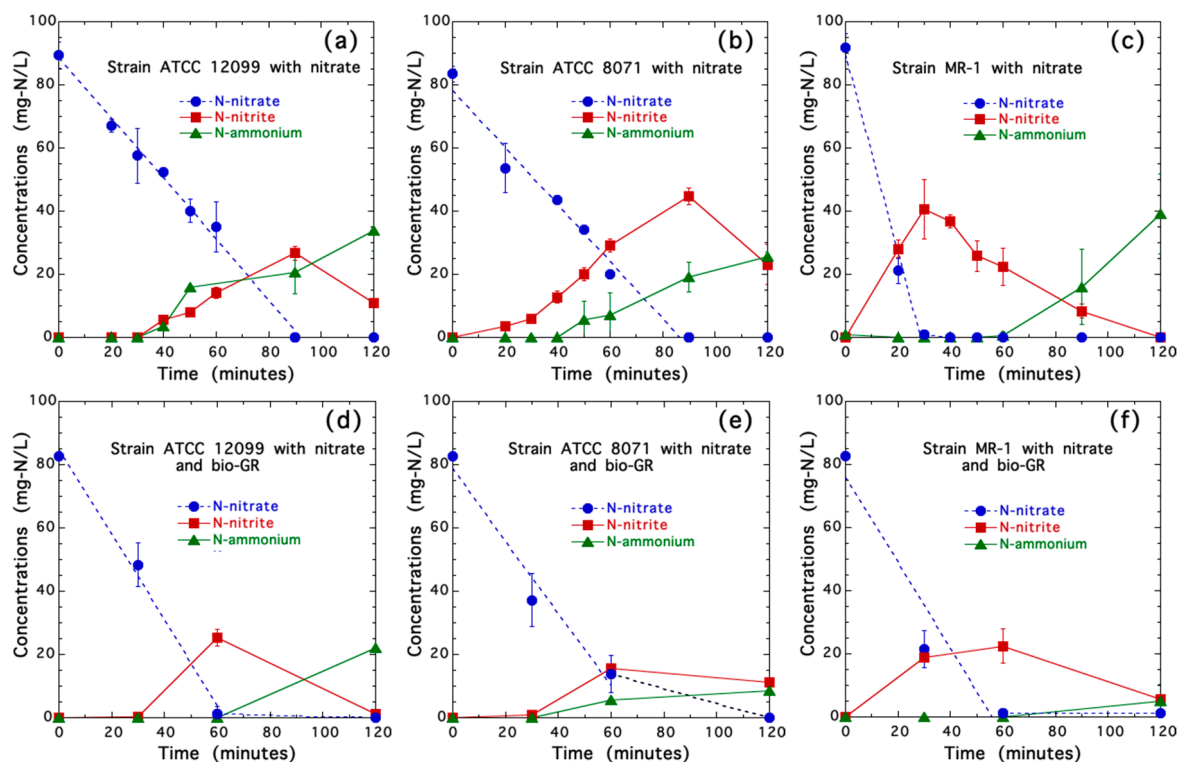


**Figure 3.** Comparison of nitrate reduction by *S. putrefaciens* ATCC 12099 (a,d), *S. putrefaciens* ATCC 8071 (b,e), and *S. oneidensis* MR-1 (c,f) in the absence (a–c) or presence (d–f) of biogenic Fe(II-III) hydroxycarbonate green rust, here referred to as “bio-GR”. All experiments were carried out in triplicate, except for those performed with strains ATCC 12009 and ATCC 8071 in the absence of bio-GR, which were in duplicate. Error bars correspond to standard deviations of replicate experiments. Dashed lines correspond to initial rates of nitrate reduction calculated using a linear regression fitting procedure in the time interval between time zero and 90 min for ATCC 12099 and ATCC 8071, between time zero and 30 min for MR-1, and between time zero and 60 min for all experiments carried out in the presence of bio-GR. Solid lines correspond to the interpolation of experimental data of nitrite and ammonium.

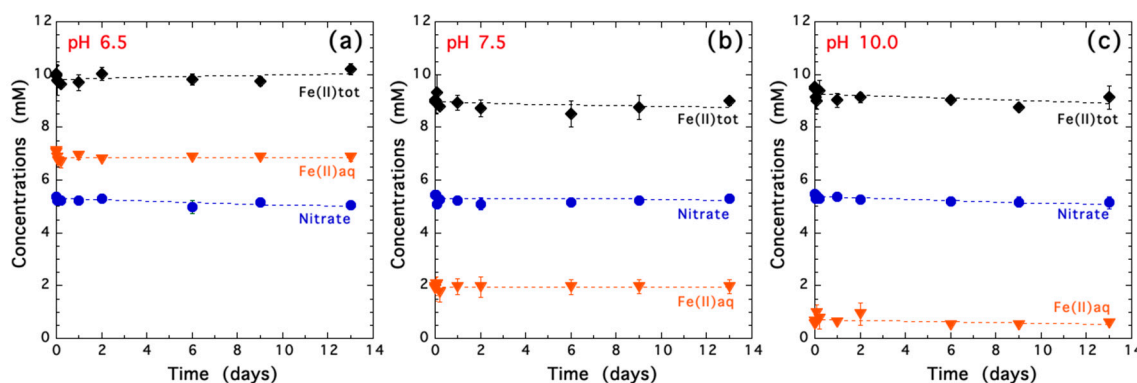


**Figure 4.** Abiotic nitrate (in blue) interaction with biogenic iron(II-III) hydroxycarbonate green rust at (a) pH 6.5; (b) pH 7.5 and (c) pH 10.0. Fe(II)tot (in black) corresponds to the total Fe(II) concentration measured by the 1,10-phenanthroline colorimetric analysis after 0.5 M HCl extraction. Fe(II)aq (in orange) corresponds to the dissolved Fe(II) concentration measured by the 1,10-phenanthroline colorimetric analysis in samples filtered through the 0.22  $\mu\text{m}$  pore size filters. Experimental data were fit using a linear regression fitting procedure (dashed lines).



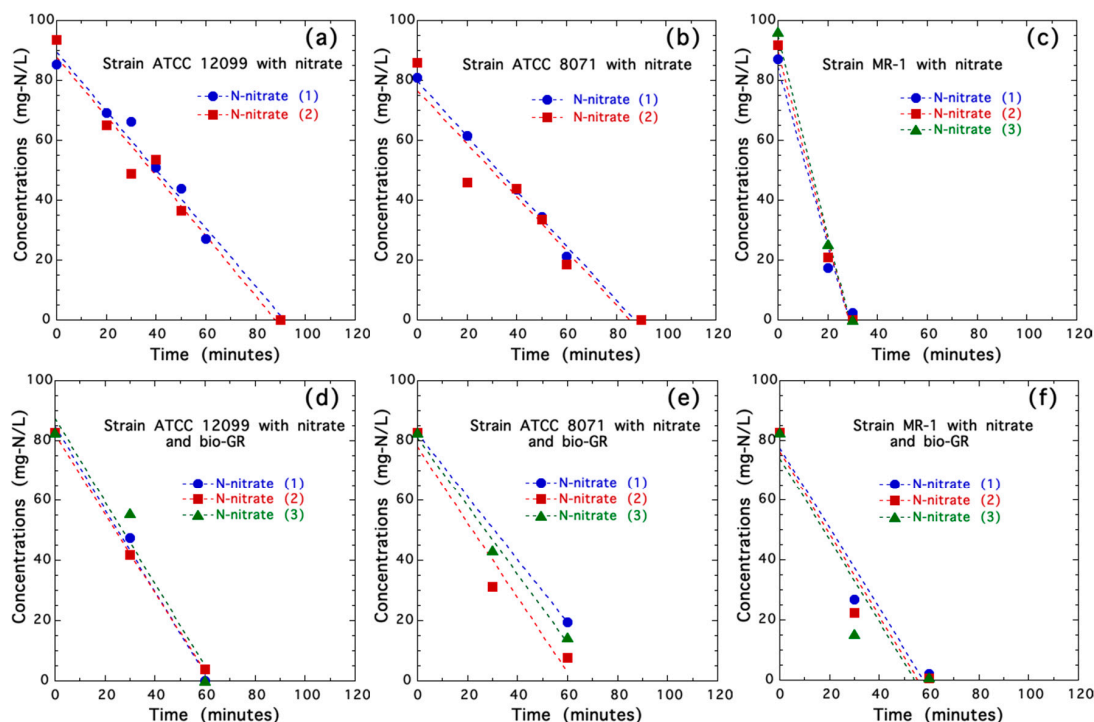


**Figure 5.** Initial rates of nitrate reduction by *S. putrefaciens* ATCC 12099 (a,d), *S. putrefaciens* ATCC 8071 (b,e), and *S. oneidensis* MR-1 (c,f) in the absence and presence of biogenic iron(II-III) hydroxycarbonate green rust. All experiments were carried out in triplicate, except for those performed with strains ATCC 12099 and ATCC 8071 in the absence of bio-GR(CO<sub>3</sub>), which were in duplicate. Error bars correspond to standard deviations of replicate experiments. Initial rates of nitrate reduction were calculated using a linear regression fitting (dashed lines) procedure in the time interval between time zero and 90 min for ATCC 12099 and ATCC 8071, between time zero and 30 min for MR-1, and between time zero and 60 min for all experiments carried out in the presence of bio-GR(CO<sub>3</sub>).

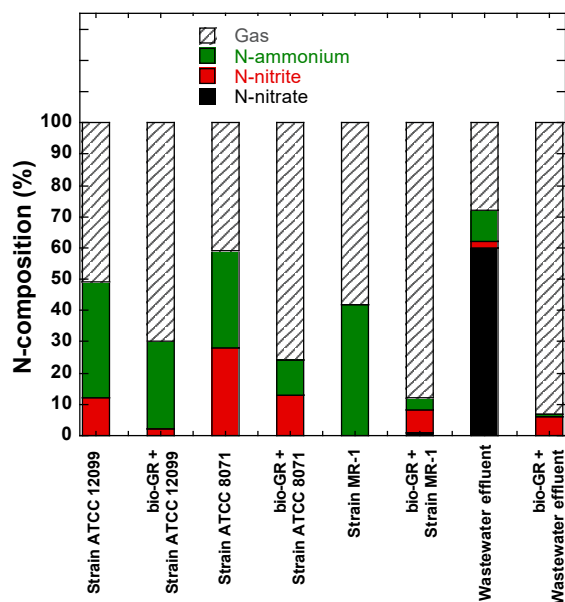


**Figure 6.** Ammonium and nitrite selectivity calculated at the end of each experiment performed with *S. putrefaciens* ATCC 12099, *S. putrefaciens* ATCC 8071, *S. oneidensis* MR-1 or with a native wastewater-denitrifying consortium after addition of nitrate ions in the absence or presence of bio-GR(CO<sub>3</sub>).

**Table 3.** Dissolved nitrogen speciation during bacterial nitrate and nitrite reduction in the presence or absence of biogenic iron (II-III) hydroxycarbonate green rust, referred to as “bio-GR(CO<sub>3</sub>)”.

Experiments Performed with Nitrate in the Starting Solution						
	X(NO <sub>3</sub> <sup>-</sup> ) <sub>t</sub> (%)	R(NH <sub>4</sub> <sup>+</sup> ) <sub>t</sub> (%)	R(NO <sub>2</sub> <sup>-</sup> ) <sub>t</sub> (%)	S(NH <sub>4</sub> <sup>+</sup> ) <sub>t</sub> (%)	S(NO <sub>2</sub> <sup>-</sup> ) <sub>t</sub> (%)	Gas (%)
<sup>1</sup> Strain ATCC 12099	100(0)	37(5)	12(1)	37(5)	12(1)	51(6)
<sup>2</sup> bio-GR(CO <sub>3</sub> ) + Strain ATCC 12099	100(0)	28(3)	2(3)	28(3)	2(3)	70(5)
<sup>1</sup> Strain ATCC 8071	100(0)	31(3)	28(9)	31(3)	28(9)	41(11)
<sup>2</sup> bio-GR(CO <sub>3</sub> ) + Strain ATCC 8071	100(0)	11(1)	13(5)	11(1)	13(5)	76(4)
<sup>2</sup> Strain MR-1	100(0)	42(12)	0(0)	42(12)	0(0)	58(12)
<sup>2</sup> bio-GR(CO <sub>3</sub> ) + Strain MR-1	99(1)	4(6)	7(2)	4(6)	7(2)	88(7)
<sup>3</sup> Wastewater influent	40	4	1	10	2	28
<sup>3</sup> bio-GR(CO <sub>3</sub> ) + Wastewater influent	100	1	6	1	6	93
Experiments Performed with Nitrite in the Starting Solution						
	X(NO <sub>2</sub> <sup>-</sup> ) <sub>t</sub> (%)	R(NH <sub>4</sub> <sup>+</sup> ) <sub>t</sub> (%)	S(NH <sub>4</sub> <sup>+</sup> ) <sub>t</sub> (%)	Gas (%)		
<sup>2</sup> Strain ATCC 12099	84(1)	51(9)	60(12)	24(13)		
<sup>2</sup> Strain ATCC 8071	74(1)	51(6)	69(6)	5(5)		
<sup>1</sup> Strain MR-1	100(0)	78(16)	78(16)	22(16)		
<sup>3</sup> Wastewater influent	42	-25	-60	n.d		
<sup>1</sup> bio-GR(CO <sub>3</sub> ) + Wastewater influent	96(3)	4(3)	5(3)	87(9)		

<sup>1</sup> Duplicate experiments; <sup>2</sup> triplicate experiments; <sup>3</sup> single experiment; mean values obtained from duplicate or triplicate experiments are indicated, with standard deviations given in parentheses.

### 3.3. Nitrite Reduction by Three Strains of *Shewanella* Species

The three *Shewanella* strains showed an ability to reduce nitrite (Figure 7), with a higher reduction rate in absolute value for *S. oneidensis* MR-1 ( $-37 \pm 1 \text{ mg-N L}^{-1} \text{ h}^{-1}$ ,  $r^2 = 0.97 \pm 0.01$ ) than for ATCC 12099 and ATCC 8071 of *S. putrefaciens* ( $-23 \pm 3 \text{ mg-N L}^{-1} \text{ h}^{-1}$ ,  $r^2 = 0.96 \pm 0.01$ ). However, these nitrite reduction rates were lower than those of nitrate reduction for the same three bacteria (see Section 3.2). The average value of ammonium selectivity obtained after 120 min of incubation from the three strains was  $69 \pm 15\%$  (Table 3); this value is about twice higher than that of the nitrate conversion into ammonium for the same incubation time in the nitrate experiments ( $37 \pm 9\%$ ) (Table 3). Our findings indicate that when nitrite is present in the starting solutions, the dominant metabolic pathway for the three *Shewanella* strains is the conversion of nitrite into ammonium (Figure 7). Finally, our experiments carried out in axenic cultures using *Shewanella* spp. showed that the three microorganisms produced a high amount of ammonium when respiring nitrate and nitrite under anoxic conditions, and that the addition of bio-GR(CO<sub>3</sub>) in such bioassays significantly decreased the selectivity of the reaction towards ammonium.

### 3.4. Nitrate and Nitrite Reduction by Autochthonous Wastewater-Denitrifying Bacteria Influent

Our results indicated that autochthonous denitrifying bacteria from a wastewater influent were capable of reducing 40% of nitrate and 42% of nitrite ions after five days of incubation in the absence of bio-GR(CO<sub>3</sub>) (Figure 8a,b; Table 3). Conversely, in the presence of bio-GR(CO<sub>3</sub>), nitrate and nitrite ions were almost fully reduced (100% and 96%, respectively) after four days of incubation (Figure 8c,d; Table 3). Results showed that in the absence of bio-GR(CO<sub>3</sub>), initial rates of nitrate and nitrite reduction were equal to  $-11.6 \text{ mg-N L}^{-1} \text{ h}^{-1}$  ( $r^2 = 0.85$ ) and  $-1.2 \text{ mg-N L}^{-1} \text{ h}^{-1}$  ( $r^2 = 0.98$ ), respectively; while in the presence of bio-GR(CO<sub>3</sub>), initial rates of nitrate and nitrite reduction were  $-1.3 \text{ mg-N L}^{-1} \text{ h}^{-1}$  ( $r^2 = 0.94$ ) and  $-2.1 \text{ mg-N L}^{-1} \text{ h}^{-1}$  ( $r^2 = 0.98$ ), respectively. The kinetics of nitrate reduction by

native wastewater-denitrifying bacteria (Figure 8a) was 9.6-fold higher than that of nitrite reduction (Figure 8c). In contrast, the presence of bio-GR(CO<sub>3</sub>) increased the kinetics of nitrite reduction to gaseous nitrogen species (Figure 8d), the corresponding value being 1.6-fold higher than that of bacterial nitrate reduction (Figure 8b). Moreover, our results revealed that the presence of bio-GR(CO<sub>3</sub>) led to a decrease in the selectivity of the reaction towards ammonium from 10% to 1% (Table 3), indicating that the association of bio-GR(CO<sub>3</sub>) with autochthonous wastewater-denitrifying bacteria efficiently promotes the removal of nitrate and nitrite, as well as the decrease of ammonium production (Figure 6). These findings suggest that such an association would result in the full conversion of nitrate ions to gaseous nitrogen species.

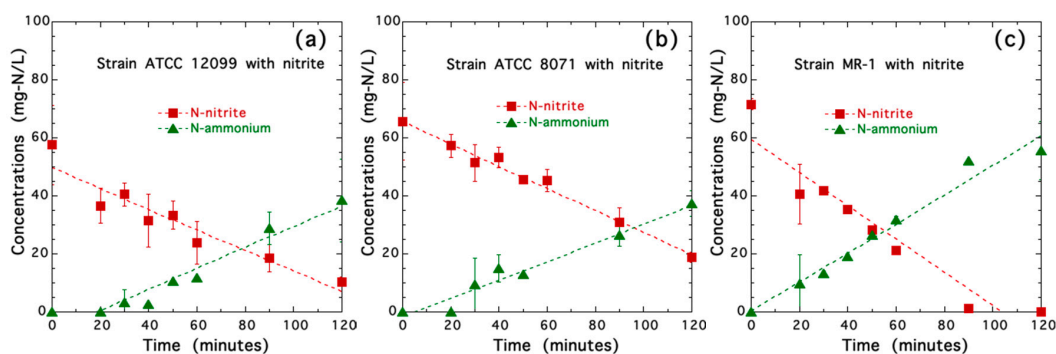


**Figure 7.** Nitrite reduction by *S. putrefaciens* ATCC 12099 (a), *S. putrefaciens* ATCC 80.71 (b) and *S. oneidensis* MR-1 (c). All experiments were performed in triplicate, except for *S. oneidensis* MR-1 for which experiments were carried out in duplicate. Error bars correspond to standard deviations of triplicate or duplicate experiments. Experimental data were fit using a linear regression model.

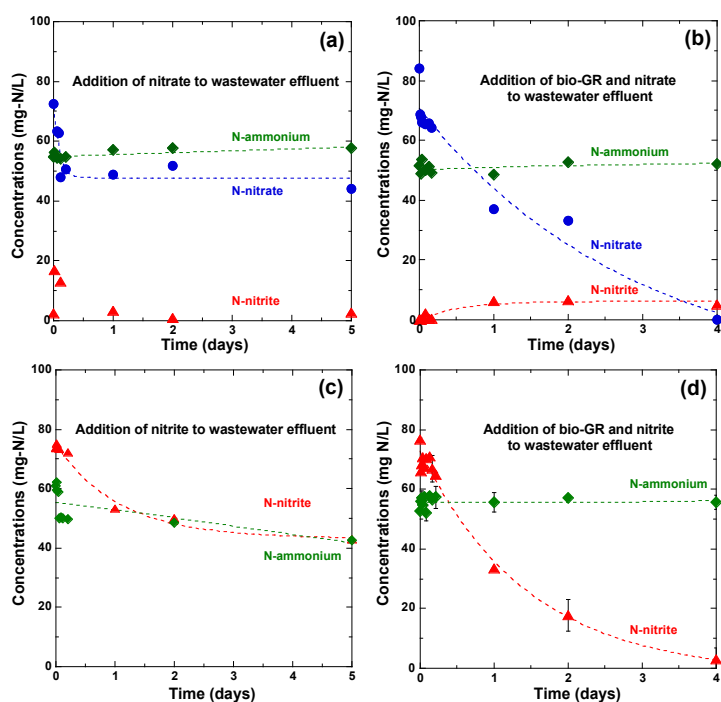


**Figure 8.** Nitrate and nitrite reduction in wastewater influent by a native wastewater-denitrifying consortium in the absence (a,c) or presence (b,d) of biogenic Fe(II-III) hydroxycarbonate green rust, referred to as “bio-GR(CO<sub>3</sub>)”. Nitrite ( $76 \pm 2 \text{ mg-N L}^{-1}$ ) and nitrate ( $78 \pm 8 \text{ mg-N L}^{-1}$ ) ions were added to wastewater influent that initially contained ammonium concentrations around  $55 \pm 4 \text{ mg-N L}^{-1}$  ( $n = 5$ ). Error bars represent standard deviation. Experimental data of nitrate and nitrite reduction (dashed lines) were fit using a pseudo-first-order kinetic model, while experimental data of ammonium were fit using a linear regression fitting procedure.

#### 4. Discussion

**Ammonium production during nitrate and nitrite reduction.** We showed that when the reduction of nitrate and nitrite ions by *S. oneidensis* MR-1 and *S. putrefaciens* (strains ATCC 12099 and ATCC 8071) is fully or nearly complete under non-growth conditions, the reaction leads to the formation of significant proportions of ammonium, resulting in ammonium selectivity of  $37 \pm 9\%$  from the initial nitrate concentration, and of  $69 \pm 15\%$  from the initial nitrite concentration, respectively. Mass balance of nitrogen species suggests the concomitant formation of gaseous nitrogen products such as  $N_2O$  and  $N_2$  in these bioassays (Reactions (2) and (3) in Figure 9). The ability of *Shewanella* species to convert nitrate into ammonium or to act as true denitrifiers is still a matter of debate. Indeed, many bacterial strains found in twelve species of the genus *Shewanella* are capable of reducing nitrate to nitrite [47].

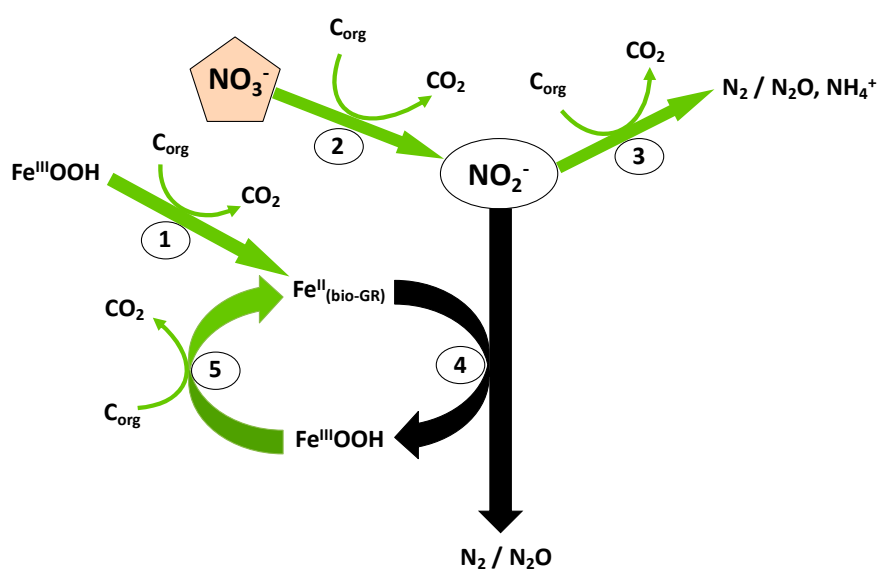


**Figure 9.** Schematic diagram presenting the coupling between bacterial nitrate reduction and abiotic nitrite conversion into gaseous nitrogen species by biogenic hydroxycarbonate green rust, referred to as “bio-GR( $CO_3$ )”. Reactions are numbered from 1 to 5: step 1: bio-GR( $CO_3$ ) formation upon reduction of ferric oxyhydroxides by *Shewanella* spp. [35]; step 2: bacterial nitrate reduction by *Shewanella* spp. or other heterotrophic bacteria inducing the accumulation of nitrite; step 3: bacterial nitrite reduction by *Shewanella* spp. or other heterotrophic bacteria into ammonium and  $N_2/N_2O$ ; step 4: abiotic nitrite reduction into gaseous nitrogen species by bio-GR( $CO_3$ ) resulting in the oxidation of structural  $Fe(II)_{\text{bio-GR}}$  to  $Fe^{III}OOH$ , which can be bacterially transformed into bio-GR( $CO_3$ ) (step 5) [41,42,44].

However, the nature of end-products resulting from nitrite reduction, i.e.,  $NH_4^+$  or  $N_2O/N_2$  is controversial and has been reported to depend on both the redox potential and the carbon-to-nitrate/nitrite ratio of the culture. Under anoxic growth conditions in nutrient-rich media, Krause and Nealson [48] observed the reduction of nitrate into  $N_2O$  by *S. oneidensis* MR-1, MR-4 and MR-7 (formerly *S. putrefaciens*) with very low ammonium production in low carbon-to-electron acceptor ratio ( $C/NO_3^-$ ) media used. By contrast, the study by Cruz-García et al. [49] demonstrated that anaerobic cultures of *S. oneidensis* MR-1 using nitrate as the sole electron acceptor, and lactate as a carbon and energy source exhibited a sequential reduction of nitrate to nitrite and then to ammonium with very low  $N_2$  and  $N_2O$  production. A previous study of nitrate reduction by *S. putrefaciens* reported that the dissimilatory pathway to either ammonium production or  $N_2$  and  $N_2O$  production (corresponding to the denitrification process) could co-exist depending on the redox potential of the culture medium [50]. According to Samuelsson [50], *S. putrefaciens* dissimilated nitrate to ammonium in media with glucose and high redox potential, while  $N_2$  and  $N_2O$  were produced at low redox potential. Accordingly, in our experiments, methanoate is introduced in excess leading to a C/N ratio of 12, which could explain that ammonium is one of the main reduction products. This is in agreement

with the study by Akunna et al. [51] that reported that ammonium production upon nitrate and nitrite reduction is favored in carbon-rich synthetic wastewaters.

**Nitrite accumulation in nitrogen removal processes.** We observed nitrite accumulation during anaerobic nitrate reduction by three *Shewanella* strains as well as by a native wastewater-denitrifying consortium (reaction 2 in Figure 9). Such a nitrite accumulation suggests that nitrite reduction into gaseous nitrogen species or ammonium was slower than the reduction of nitrate to nitrite. The levels of nitrite accumulation observed in our study are similar to those previously reported during nitrate reduction by *S. oneidensis* MR-1, MR-4 and MR-7 [48,49], *S. putrefaciens* 200 [52], and *Paracoccus denitrificans* [53]. Nitrite accumulation is also frequently observed in natural media such as river sediments [54] or in activated sludge [9,55]. The causes of nitrite accumulation have been previously discussed. Betlach and Tiedje [56] proposed an explanation based on the kinetics of nitrate versus nitrite reduction. They demonstrated that lower nitrite reduction rates compared to nitrate reduction rates in cultures of *Alcaligenes* species and *Pseudomonas fluorescens* were responsible for nitrite accumulation. This is in agreement with our results that indicated that nitrite reduction rates were lower than those of nitrate reduction. Such lower reduction rates for nitrite than for nitrate could explain the accumulation of nitrite during the bacterial nitrate reduction, suggesting a possible competition between nitrite reductase and nitrate reductase with respect to electron transfer. Moreover, we observe that nitrite accumulation is clearly different for the three *Shewanella* strains when incubated with a carbon-to-electron acceptor ratio equal to 12 under the same culture conditions, supporting that nitrate reduction activities of the three *Shewanella* strains used were different from each other. Our findings agree with the study by Ge et al. [55] that showed that increased COD/NO<sub>3</sub><sup>-</sup> ratio favors nitrite accumulation and that proposed that nitrite accumulation could be induced by a competition for electrons between nitrite reductase and nitrate reductase, resulting in different reduction rates for nitrite and nitrate. Our study suggests also that each of the three *Shewanella* strains used has a distinct nitrate reduction activity. Additionally, the extent of nitrite accumulation depends on bacterial species [57]. Overall our study clearly shows that the reduction of nitrite in the absence of nitrate in the starting solution is lower than that of nitrate under the similar conditions. This observation is confirmed by results obtained on experiments carried out with the three bacterial species and supports a kinetic explanation for nitrite accumulation upon heterotrophic nitrate reduction. Moreover, our results reveal that the accumulation of nitrite ions was overall lower in the presence of biogenic Fe(II-III) hydroxycarbonate green rust than in its absence, suggesting that bio-GR(CO<sub>3</sub>) reduces a fraction of nitrite into gaseous nitrogen species, as shown in our previous study [35], while another fraction of nitrite is reduced by bacteria into ammonium.

**Biogenic hydroxycarbonate green rust: a good candidate for denitrification.** As detailed in the previous section, nitrite plays an important role in modern nitrogen removal processes. Much attention is thus paid at controlling the products of nitrite reduction in such processes. In a previous study, we demonstrated that biogenic mixed-valent iron(II-III) hydroxycarbonate green rust, bio-GR(CO<sub>3</sub>) was able to rapidly decrease the selectivity of the nitrite reduction reaction towards ammonium under abiotic conditions [41]. Here we demonstrated that bio-GR(CO<sub>3</sub>) significantly reduces ammonium production during the nitrite reduction step upon bacterial nitrate reduction. This decrease in ammonium selectivity is explained by the ability of bio-GR(CO<sub>3</sub>) to rapidly convert nitrite into gaseous nitrogen species, which competes with a lower bacterial nitrite reduction to ammonium in our experiments. Figure 9 summarizes the reactions involved in this coupling between bacterial nitrate reduction and abiotic nitrite reduction by biogenic bio-GR(CO<sub>3</sub>). In this new biologically-assisted mineral denitrification process in aqueous solution, the bacterial conversion of nitrate into nitrite is coupled to the oxidation of organic carbon to carbon dioxide, nitrite is then reduced abiotically by biogenic green rust without additional carbon requirement. Such a coupling of biotic and abiotic reactions could thus be potentially applied for denitrifying low carbon content wastewater.

Our results show that bio-GR(CO<sub>3</sub>) does not react with nitrate. This result is surprising because green rusts are capable of readily reducing nitrite ions and because previous studies have shown



that synthetic green rusts are capable of reducing nitrate to ammonium. This latter reaction was performed with abio-GR(SO<sub>4</sub>) [39], abio-GR(Cl) [40] and abio-GR(F) [38], which were more ferrous than the bio-GR(CO<sub>3</sub>) samples used in the present study. In a previous study by Hansen et al. [40], the reduction of nitrate to ammonium was coupled to the oxidation of green rust to magnetite; the most ferrous green rust, i.e., abio-GR(Cl) having an Fe(II)/Fe(III) ratio equal to 3, reacted much faster than the less ferrous ones, abio-GR(SO<sub>4</sub>) and abio-GR(CO<sub>3</sub>) for which the Fe(II)/Fe(III) ratio was 2. Hence it can be inferred such chemically synthesized green rusts are not suitable for denitrification because they replace nitrate by a significant amount of ammonium. In contrast, the biogenic hydroxycarbonate green rust used in our study cannot react directly with nitrate ions at pH ranging from 6.5 to 10.0. This lack of reactivity is assigned to the low Fe(II) content in these bio-GR(CO<sub>3</sub>) particles as their Fe(II)/Fe(III) ratios ranged from 1 to 1.2 [41]. This suggests that the reaction between nitrate ions and dissolved Fe(II) is negligible in the 6.5 to 10.0 pH-range and for incubation times of 13 days. However, bio-GR(CO<sub>3</sub>) reduces nitrite ions without ammonium production [41] and can thus effectively be associated to the first step of biological denitrification that converts nitrate to nitrite. The formation of nitrite is a central step in nitrogen biogeochemical cycling, including denitrification, DNRA and nitrification processes. Nitrification is the first step in the removal of nitrogen in domestic wastewater treatments. Ruiz et al. [58] studied the optimal conditions to favor partial biological nitrification-denitrification process via nitrite instead of nitrate. These authors showed that partial nitrification resulting in high nitrite accumulation was possible by decreasing the dissolved oxygen concentration in the nitrification step and that denitrification can take place directly from nitrite instead of from nitrate. The advantages of such a process are to decrease the oxygen and carbon demands and to decrease the production of sludge [58,59]. This process is considered an operational strategy that can be applied on preexisting industrial installations, and it could be complementary to our biologically assisted mineral denitrification process. It has also inspired newly developed processes such as the completely autotrophic nitrogen removal over nitrite (CANON) [31,60,61], as well as the single reactor system high activity ammonium removal over nitrite (SHARON) [62] that are proposed for the treatment of water with a low organic carbon content typical of wastewater treatment plants (WWTP). On the basis of nitrite reactivity, bacterial anaerobic ammonium oxidation (ANAMMOX) is also useful in such contexts [63,64].

**Author Contributions:** Conceptualization, G.O.-N., D.G. and G.M.; methodology, G.O.-N., J.B. and D.G.; validation, G.O.-N., D.G., C.P., M.A. and G.M.; formal analysis, D.G., M.A., J.B. and G.O.-N.; M.A.; investigation, G.O.-N., D.G., G.M., J.B., C.P., and M.A.; data curation, G.O.-N., D.G., G.M., J.B., C.P., and M.A.; writing—original draft preparation, G.O.-N., D.G., G.M. and C.P.; writing—review and editing, G.O.-N., G.M., M.A. and C.P.; supervision, G.O.-N., and G.M. All authors have read and agreed to the published version of the manuscript.

**Funding:** This research was funded by the Ecotech program of the “Agence Nationale de la Recherche” (ANR) for 89.3%, piloted by ADEME (ECOTECH2009–No. 0994C0103), and by SAUR for 10.7%.

**Acknowledgments:** The authors acknowledge SAUR for the wastewater used in the study.

**Conflicts of Interest:** The authors declare no conflict of interest. The funders had no role in the design of the study; in the analyses, or interpretation of data; in the writing of the manuscript, or in the decision to publish the results.

## References

1. Philips, S.; Laanbroek, H.J.; Verstraete, W. Origin, causes and effects of increased nitrite concentrations in aquatic environments. *Rev. Environ. Sci. Biotechnol.* **2002**, *1*, 115–141. [[CrossRef](#)]
2. Lorenz, M.C. A marriage of old and new: Chemostats and microarrays identify a new model system for ammonium toxicity. *PLoS Biol.* **2006**, *4*, 1905–1907. [[CrossRef](#)] [[PubMed](#)]
3. Shinn, C.; Marco, A.; Serrano, L. Influence of low levels of water salinity on toxicity of nitrite to anuran larvae. *Chemosphere* **2013**, *92*, 1154–1160. [[CrossRef](#)] [[PubMed](#)]
4. Esteban, R.; Arizb, I.; Cruzb, C.; Moran, J.F. Review: Mechanisms of ammonium toxicity and the quest for tolerance. *Plant Sci.* **2016**, *248*, 92–101. [[CrossRef](#)] [[PubMed](#)]
5. Cloern, J.E. Our evolving conceptual model of the coastal eutrophication problem. *Mar. Ecol. Prog. Ser.* **2001**, *210*, 223–253. [[CrossRef](#)]

6. Teichberg, M.; Fox, S.E.; Olsen, Y.S.; Valiela, I.; Martinetto, P.; Iribarne, O.; Yuriko Muto, E.; Petti, M.A.V.; Corbisier, T.N.; Soto-Jiménez, M.; et al. Eutrophication and macroalgal blooms in temperate and tropical coastal waters: Nutrient enrichment experiments with *Ulva* spp. *Glob. Chang. Biol.* **2010**, *16*, 2624–2637. [[CrossRef](#)]
7. Akunna, J.C.; Bizeau, C.; Moletta, R. Nitrate and nitrite reductions with anaerobic sludge using various carbon sources: Glucose, glycerol, acetic acid, lactic acid and methanol. *Water Res.* **1993**, *27*, 1303–1312. [[CrossRef](#)]
8. Foglar, L.; Briski, F.; Sipos, L.; Vuković, M. High nitrate removal from synthetic wastewater with the mixed bacterial culture. *Bioresour. Technol.* **2005**, *96*, 879–888. [[CrossRef](#)]
9. Glass, C.; Silverstein, J. Denitrification kinetics of high nitrate concentration water: pH effect on inhibition and nitrite accumulation. *Water Res.* **1998**, *32*, 831–839. [[CrossRef](#)]
10. Khan, A.; Ayub, M.; Khan, W.M. Hyperammonemia is associated with increasing severity of both liver cirrhosis and hepatic encephalopathy. *Int. J. Hepatol.* **2016**, *2016*, doi. [[CrossRef](#)]
11. De Lucas, A.; Rodríguez, L.; Villaseñor, J.; Fernández, F.J. Denitrification potential of industrial wastewaters. *Water Res.* **2005**, *39*, 3715–3726. [[CrossRef](#)]
12. Rajagopal, R.; Saady, N.M.C.; Torrijos, M.; Thanikal, J.V.; Hung, Y.-T. Sustainable agro-food industrial wastewater treatment using high rate anaerobic process. *Water* **2013**, *5*, 292–311. [[CrossRef](#)]
13. Gander, M.; Jefferson, B.; Judd, S. Aerobic MBRs for domestic wastewater treatment: A review with cost considerations. *Sep. Purif. Technol.* **2000**, *18*, 119–130. [[CrossRef](#)]
14. Zakkour, P.D.; Gaterell, M.R.; Griffin, P.; Gochin, R.J.; Lester, J.N. Anaerobic treatment of domestic wastewater in temperate climates: Treatment plant modelling with economic considerations. *Water Res.* **2001**, *35*, 4137–4149. [[CrossRef](#)]
15. Aiyuk, S.; Odonkor, P.; Theko, N.; van Haandel, A.; Verstraete, W. Technical problems ensuing from UASB reactor application in domestic wastewater treatment without pre-treatment. *Int. J. Environ. Sci. Dev.* **2010**, *1*, 392–398. [[CrossRef](#)]
16. Kassab, G.; Halalsheh, M.; Klapwijk, A.; Fayyad, M.; van Lier, J.B. Sequential anaerobic–aerobic treatment for domestic wastewater—A review. *Bioresour. Technol.* **2010**, *101*, 3299–3310. [[CrossRef](#)]
17. Sani, A.; Scholz, M.; Bouillon, L. Seasonal assessment of experimental vertical-flow constructed wetlands treating domestic wastewater. *Bioresour. Technol.* **2013**, *147*, 585–596. [[CrossRef](#)]
18. Bestawy, E.E.; AL-Hejin, A.; Amer, R.; Kashmeri, R.A. Decontamination of domestic wastewater using suspended individual and mixed bacteria in batch system. *J. Bioremediat. Biodegrad.* **2014**, *5*, 1–8. [[CrossRef](#)]
19. Subtil, E.L.; Mierzwa, J.C.; Hespagnol, I. Comparison between a conventional membrane bioreactor (c-MBR) and a biofilm membrane bioreactor (bf-MBR) for domestic wastewater treatment. *Braz. J. Chem. Eng.* **2014**, *31*, 683–691. [[CrossRef](#)]
20. Nasr, F.A.; Mikhaeil, B. Treatment of domestic wastewater using modified septic tank. *Desalin. Water Treat.* **2014**, *56*, 2073–2081. [[CrossRef](#)]
21. Nasr, F.A.; Doma, H.S.; Abdel-Halim, H.S.; El-Shafai, S.A. Chemical industry wastewater treatment. *TESCE* **2004**, *30*, 1183–1206. [[CrossRef](#)]
22. Zhou, Y.-F.; Liu, M.; Wu, Q. Water quality improvement of a lagoon containing mixed chemical industrial wastewater by micro-electrolysis-contact oxidization. *Appl. Phys. Eng.* **2011**, *12*, 390–398. [[CrossRef](#)]
23. Shinde, S.S.; Bhosale, C.H.; Rajpure, K.Y. Hydroxyl radical's role in the remediation of wastewater. *J. Photochem. Photobiol. B* **2012**, *116*, 66–74. [[CrossRef](#)] [[PubMed](#)]
24. Rodrigues, C.S.D.; Madeira, L.M.; Boaventura, R.A.R. Decontamination of an industrial cotton dyeing wastewater by chemical and biological processes. *Ind. Eng. Chem. Res.* **2014**, *53*, 2412–2421. [[CrossRef](#)]
25. Shrimali, M.; Singh, K.P. New methods of nitrate removal from water. *Environ. Pollut.* **2001**, *112*, 351–359. [[CrossRef](#)]
26. Wei, C.; Zhang, T.; Feng, C.; Wu, H.; Deng, Z.; Wu, C.; Lu, B. Treatment of food processing wastewater in a full-scale jet biogas internal loop anaerobic fluidized bed reactor. *Biodegradation* **2011**, *22*, 347–357. [[CrossRef](#)]
27. Rupani, P.F.; Singh, R.P.; Ibrahim, M.H.; Esa, N. Review of current palm oil mill effluent (POME) treatment methods: Vermicomposting as a sustainable practice. *World Appl. Sci. J.* **2010**, *10*, 1190–1201.
28. Gotmare, M.; Dhoble, R.M.; Pittule, A.P. Biomethanation of dairy waste water through UASB at mesophilic temperature range. *Int. J. Adv. Eng. Sci. Technol.* **2011**, *8*, 1–9.

29. Passeggi, M.; Lopez, I.; Borzacconi, L. Integrated anaerobic treatment of dairy industrial wastewater and sludge. *Water Sci. Technol.* **2009**, *59*, 501–506. [[CrossRef](#)]
30. Senturk, E.; Ince, M.; Engin, O.G. Treatment efficiency and VFA composition of a thermophilic anaerobic contact reactor treating food industry wastewater. *J. Hazard. Mater.* **2010**, *176*, 843–848. [[CrossRef](#)]
31. Sun, G.; Austin, D. Completely autotrophic nitrogen-removal over nitrite in lab-scale constructed wetlands: Evidence from a mass balance study. *Chemosphere* **2007**, *68*, 1120–1128. [[CrossRef](#)] [[PubMed](#)]
32. Westerhoff, P.; James, J. Nitrate removal in zero-valent iron packed columns. *Water Res.* **2003**, *37*, 1818–1830. [[CrossRef](#)]
33. Rodríguez-Maroto, J.M.; García-Herruzo, F.; García-Rubio, A.; Gómez-Lahoz, C.; Vereda-Alonso, C. Kinetics of the chemical reduction of nitrate by zero-valent iron. *Chemosphere* **2009**, *74*, 804–809. [[CrossRef](#)]
34. Zhang, J.; Hao, Z.; Zhang, Z.; Yang, Y.; Xu, X. Kinetics of nitrate reductive denitrification by nanoscale zero-valent iron. *Process Saf. Environ. Prot.* **2010**, *88*, 439–445. [[CrossRef](#)]
35. Ryu, A.; Jeong, S.-W.; Jang, A.; Choi, H. Reduction of highly concentrated nitrate using nanoscale zero-valent iron: Effects of aggregation and catalyst on reactivity. *Appl. Catal. B* **2011**, *105*, 128–135. [[CrossRef](#)]
36. Choe, S.; Liljestrand, H.M.; Khim, J. Nitrate reduction by zero-valent iron under different pH regimes. *Appl. Geochem.* **2004**, *19*, 335–342. [[CrossRef](#)]
37. Van Nooten, T.; Springael, D.; Bastiaens, L. Positive impact of microorganisms on the performance of laboratory-scale permeable reactive iron barriers. *Environ. Sci. Technol.* **2008**, *42*, 1680–1686. [[CrossRef](#)]
38. Choi, J.; Batchelor, B. Nitrate reduction by fluoride green rust modified with copper. *Chemosphere* **2008**, *70*, 1108–1116. [[CrossRef](#)]
39. Hansen, H.C.B.; Koch, C.B.; Nancke-Krogh, H.; Borggaard, O.K.; Sorensen, J. Abiotic nitrate reduction to ammonium: Key role of green rust. *Environ. Sci. Technol.* **1996**, *30*, 2053–2056. [[CrossRef](#)]
40. Hansen, H.C.B.; Guldberg, S.; Erbs, M.; Koch, C.B. Kinetics of nitrate reduction by green rusts—Effects of interlayer anion and Fe(II):Fe(III) ratio. *Appl. Clay Sci.* **2001**, *18*, 81–91. [[CrossRef](#)]
41. Guerbois, D.; Ona-Nguema, G.; Morin, G.; Abdelmoula, M.; Laverman, A.L.; Mouchel, J.-M.; Barthelemy, K.; Maillot, F.; Brest, J. Nitrite reduction by biogenic hydroxycarbonate green rusts: Evidence for hydroxy-nitrite green rust formation as intermediate reaction product. *Environ. Sci. Technol.* **2014**, *48*, 4505–4514. [[CrossRef](#)]
42. Ona-Nguema, G.; Abdelmoula, M.; Jorand, F.; Benali, O.; Géhin, A.; Block, J.-C.; Génin, J.-M.R. Iron(II,III) hydroxycarbonate green rust formation and stabilisation from lepidocrocite bioreduction. *Environ. Sci. Technol.* **2002**, *36*, 16–20. [[CrossRef](#)]
43. Ona-Nguema, G.; Carteret, C.; Benali, O.; Abdelmoula, M.; Génin, J.-M.R.; Jorand, F. Competitive formation of hydroxycarbonate green rust 1 versus hydroxysulphate green rust 2 in *Shewanella putrefaciens* cultures. *Geomicrobiol. J.* **2004**, *21*, 79–90. [[CrossRef](#)]
44. Ona-Nguema, G.; Morin, G.; Wang, Y.; Menguy, N.; Juillot, F.; Olivi, L.; Aquilanti, G.; Abdelmoula, M.; Ruby, C.; Bargar, J.R.; et al. Arsenite sequestration at the surface of nano-Fe(OH)<sub>2</sub>, ferrous-carbonate hydroxide, and green-rust after bioreduction of arsenic-sorbed lepidocrocite by *Shewanella putrefaciens*. *Geochim. Cosmochim. Acta* **2009**, *73*, 1359–1381. [[CrossRef](#)]
45. Fadrus, H.; Maly, J. Suppression of iron(III) interference in the determination of iron(II) in water by the 1,10-phenanthroline method. *Analyst* **1975**, *100*, 549–554. [[CrossRef](#)]
46. Ruby, C.; Naille, S.; Ona-Nguema, G.; Morin, G.; Mallet, M.; Guerbois, D.; Barthélémy, K.; Etique, M.; Zegeye, A.; Zhang, Y.; et al. Use of ferrihydrite-coated pozzolana and biogenic green rust to purify wastewater containing phosphate and nitrate. *Curr. Org. Chem.* **2016**, *6*, 100–118.
47. Venkateswaran, K.; Moser, D.P.; Dollhopf, M.E.; Lies, D.P.; Saffarini, D.A.; MacGregor, B.J.; Ringelberg, D.B.; White, D.C.; Nishijima, M.; Sano, H.; et al. Polyphasic taxonomy of the genus *Shewanella* and description of *Shewanella oneidensis* sp. nov. *Int. J. Syst. Bacteriol.* **1999**, *49*, 705–724. [[CrossRef](#)] [[PubMed](#)]
48. Krause, B.; Nealson, K.H. Physiology and enzymology involved in denitrification by *Shewanella putrefaciens*. *Appl. Environ. Microbiol.* **1997**, *63*, 2613–2618. [[CrossRef](#)] [[PubMed](#)]
49. Cruz-García, C.; Murray, A.E.; Klappenbach, J.A.; Stewart, V.; Tiedje, J.M. Respiratory nitrate ammonification by *Shewanella oneidensis* MR-1. *J. Bacteriol.* **2007**, *189*, 656–662. [[CrossRef](#)]
50. Samuelsson, M.-O. Dissimilatory nitrate reduction to nitrite, nitrous oxide, and ammonium by *Pseudomonas putrefaciens*. *Appl. Environ. Microbiol.* **1985**, *50*, 812–815. [[CrossRef](#)]
51. Akunna, J.C.; Bizeau, C.; Moletta, R. Denitrification in anaerobic digesters: Possibilities and influence of wastewater COD/N-NO<sub>x</sub> ratio. *Environ. Technol.* **1992**, *13*, 825–836. [[CrossRef](#)]

52. Cooper, D.C.; Picardal, F.W.; Schimmelmann, A.; Coby, A.J. Chemical and biological interactions during nitrate and goethite reduction by *Shewanella putrefaciens* 200. *Appl. Environ. Microbiol.* **2003**, *69*, 3517–3525. [[CrossRef](#)] [[PubMed](#)]
53. Blaszczyk, M. Effect of medium composition on the denitrification of nitrate by *Paracoccus denitrificans*. *Appl. Environ. Microbiol.* **1993**, *59*, 3951–3953. [[CrossRef](#)] [[PubMed](#)]
54. Kelso, B.; Smith, R.V.; Laughlin, R.J.; Lennox, S.D. Dissimilatory nitrate reduction in anaerobic sediments leading to river nitrite accumulation. *Appl. Environ. Microbiol.* **1997**, *63*, 4679–4685. [[CrossRef](#)]
55. Ge, S.; Peng, Y.; Wang, S.; Lu, C.; Cao, X.; Zhu, Y. Nitrite accumulation under constant temperature in anoxic denitrification process: The effects of carbon sources and COD/NO(3)-N. *Bioresour. Technol.* **2012**, *114*, 137–143. [[CrossRef](#)]
56. Betlach, M.R.; Tiedje, J.M. Kinetic explanation for accumulation of nitrite, nitric oxide, and nitrous oxide during bacterial denitrification. *Appl. Environ. Microbiol.* **1981**, *42*, 1074–1084. [[CrossRef](#)] [[PubMed](#)]
57. Lazarova, V.; Capdeville, B.; Nikolov, L. Influence of seeding conditions on nitrite accumulation in a denitrifying fluidized bed reactor. *Water Res.* **1994**, *28*, 1189–1197. [[CrossRef](#)]
58. Ruiz, G.; Jeison, D.; Rubilar, O.; Ciudad, G.; Chamy, R. Nitrification-denitrification via nitrite accumulation for nitrogen removal from wastewaters. *Bioresour. Technol.* **2006**, *97*, 330–335. [[CrossRef](#)]
59. Fan, J.; Wang, W.; Zhang, B.; Guo, Y.; Ngo, H.H.; Guo, W.; Zhang, J.; Wu, H. Nitrogen removal in intermittently aerated vertical flow constructed wetlands: Impact of influent COD/N ratios. *Bioresour. Technol.* **2013**, *143*, 461–466. [[CrossRef](#)]
60. Third, K.A.; Olav Sliemers, A.; Kuenen, J.G.; Jetten, M.S.M. The CANON System (Completely Autotrophic Nitrogen-removal Over Nitrite) under ammonium limitation interaction and competition. *Syst. Appl. Microbiol.* **2001**, *24*, 588–596. [[CrossRef](#)]
61. Chang, X.; Li, D.; Liang, Y.; Yang, Z.; Cui, S.; Liu, T.; Zeng, H.; Zhang, J. Performance of a completely autotrophic nitrogen removal over nitrite process for treating wastewater with different substrates at ambient temperature. *J. Environ. Sci.* **2013**, *25*, 688–697. [[CrossRef](#)]
62. Mosquera-Corral, A.; González, F.; Campos, J.L.; Méndez, R. Partial nitrification in a SHARON reactor in the presence of salts and organic carbon compounds. *Process Biochem.* **2005**, *40*, 3109–3118. [[CrossRef](#)]
63. Hu, Z.; Lotti, T.; van Loosdrecht, M.; Kartal, B. Nitrogen removal with the anaerobic ammonium oxidation process. *Biotechnol. Lett.* **2013**, *35*, 1145–1154. [[CrossRef](#)] [[PubMed](#)]
64. Strous, M.; Van Gerven, E.; Zheng, P.; Kuenen, J.G.; Jetten, M.S.M. Ammonium removal from concentrated waste streams with the anaerobic ammonium oxidation (Anammox) process in different reactor configurations. *Water Res.* **1997**, *31*, 1955–1962. [[CrossRef](#)]



© 2020 by the authors. Licensee MDPI, Basel, Switzerland. This article is an open access article distributed under the terms and conditions of the Creative Commons Attribution (CC BY) license (<http://creativecommons.org/licenses/by/4.0/>).